

# Experimental Observation of Nonlocal Electron Thermal Transport in NSTX RF-heated L-mode plasmas

EXC

Y. Ren<sup>1</sup>, B. P. LeBlanc<sup>1</sup>, W. Guttenfelder<sup>1</sup>, S.M. Kaye<sup>1</sup>, E. Mazzucato<sup>1</sup>, K.C. Lee<sup>2</sup>, C.W. Domier<sup>3</sup>, R. E. Bell<sup>1</sup>, H. Yuh<sup>4</sup> and the NSTX Team  
(Email: yren@pppl.gov)

<sup>1</sup> Princeton Plasma Physics Laboratory, Princeton University, Princeton, NJ 08543

<sup>2</sup> National Fusion Research Institute, Daejeon, 305-806, Korea

<sup>3</sup> University of California at Davis, Davis, CA 95616

<sup>4</sup> Nova Photonics, Inc., Princeton, NJ 08540

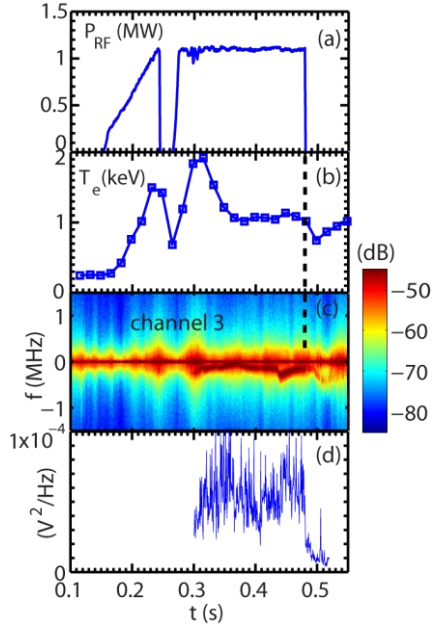


**Figure 1** The time traces of (a) injected RF power and (b) maximum  $T_e$ ; (c) Spectrogram of signal from the channel 3 of the high- $k$  scattering system; (d) Time trace of the peak spectral power of the scattered signal. A black vertical solid line extends from (b) to (c) denotes the time point at which the RF heating is terminated. i.e.  $t=479.6$  ms.

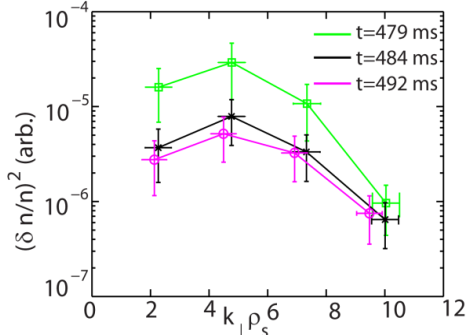


**Figure 2** The local  $k$  spectra at  $t=479$  ms (before RF cessation), 484 and 492 ms (after RF cessation) at  $R \approx 133$  to  $137$  cm ( $r/a \approx 0.57-0.63$ ) measured by the scattering system.

Understanding electron thermal transport is crucial for improving the confinement performance of future devices, e.g. FNSF and ITER, where electron heating will likely be dominant. Nonlocality in electron thermal transport has been observed in both tokamaks and stellarators [1,2], where the response of heat flux and local turbulence to external perturbation is much faster than that of local equilibrium temperature/gradients. Here, we present the first experimental observation of nonlocal electron thermal transport in NSTX. The observations were made at the times of RF cessation in a set of NSTX RF-heated L-mode plasma with  $B_T=5.5$  kG and  $I_p=300$  kA. Local electron-scale turbulence was measured with a 280 GHz collective microwave scattering system (the high- $k$  scattering system) with a fine radial localization of  $\pm 2$  cm [4], and the scattering system was configured to measure turbulence for a  $k_{\perp} \rho_s$  range of about 2 to 10 at  $R \approx 133$  to  $137$  cm ( $r/a \approx 0.57-0.63$ ). We will present results from a typical shot 140301 for which we have carried out extensive analysis.

In Fig. 1(a), it can be seen that the peak injected RF power is about 1 MW and the RF heating terminates at  $t=479.6$  ms (denoted by a vertical solid line in Fig. 1). The maximum  $T_e$  measured by a Thomson scattering system [5] is plotted in Fig. 1(b), and it is clearly seen that the maximum  $T_e$  drops after the RF power terminates. The spectrogram of the signal from channel 3 of the scattering system is shown in Fig. 1(c). The scattered signal, i.e. the spectral peaks at  $f < 0$  shown in Fig. 1(c), can be distinguished easily from the stray radiation, i.e. the central peak at  $f=0$ , from about  $t=300$  ms to 550 ms, and we can see that a sudden drop in scattered signal power at almost the same time as the RF cessation at  $t=479.6$  ms. This drop can be seen more clearly in Fig. 1(d), where the time trace of the peak spectral power of the scattered signal in Fig. 1(c) is plotted. A closer examination shows that

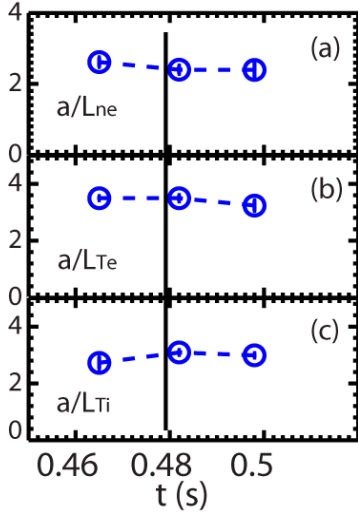


**Figure 3** Temporal evolution of local normalized electron density,  $T_e$  and  $T_i$  gradients ( $a/L_{n_e}$ ,  $a/L_{T_e}$  and  $a/L_{T_i}$ ) at three exact Thomson measurement time points. The vertical solid line denotes the time of the RF cessation.

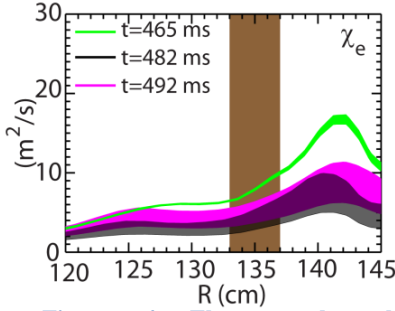


**Figure 4** Electron thermal diffusivity,  $\chi_e$ , at  $t=465$  ms (about 14 ms before RF cessation), 482 and 498 ms (after RF cessation) plotted as colored bands with vertical width denoting standard deviation. The rectangular shaded region denotes the measurement region of the high- $k$  scattering system.

this sudden drop in the turbulence spectral power and the cessation of the RF heating are not exactly synchronized: the drop in the spectral power happens approximately 1-2 ms after the RF cessation and the drop happens in about 0.5-1 ms. The change in the electron-scale turbulence wavenumber spectrum can be seen in Fig. 2, where the wavenumber spectra at  $t=479$  ms (right before the RF cessation), 484 and 492 ms (after the RF cessation) are plotted. Note that although after the RF cessation the turbulence spectral power varies little from  $t=484$  to 492 ms, the drop in the spectral power is up to about a factor of 7 from  $t=479$  ms (right before the RF cessation) to 484/492 ms (after the RF cessation).

Since the 0.5-1 ms time scale during which the turbulence spectral power drops is much smaller than the confinement time ( $\sim 10$  ms), the local equilibrium profiles are not expected to significantly change. Thus such the sudden drop in turbulence spectral power is unlikely due to variations in the local equilibrium gradients. In addition, as seen in Fig. 3, the normalized density,  $T_e$  and  $T_i$  gradients ( $a/L_{n_e}$ ,  $a/L_{T_e}$  and  $a/L_{T_i}$ ) show small changes ( $\lesssim 15\%$ ) from  $t=465$  ms (about 14 ms before the RF cessation) to 498 ms (right after the RF cessation). We note that local linear stability analyses using GS2 gyrokinetic code [6] have shown that the profiles are not close to marginal stability and ion and electron-scale instabilities are robustly unstable before and right after the RF cessation in these plasmas. Electron thermal transport was evaluated with TRANSP transport analysis code [7] coupled with TORIC calculation for the RF heating profile, and electron thermal diffusivity,  $\chi_e$ , profiles at the same three exact Thomson measurement time points as used in Fig. 3 are plotted in Fig. 4 where a factor of 2 decrease in  $\chi_e$  can be seen after the RF cessation ( $t=482/498$  ms). Such a drop in  $\chi_e$  is correlated with

the sudden drop in electron-scale turbulence spectral power shown in Fig. 2 but not correlated with the variations in the local equilibrium gradients, demonstrating the nonlocal nature of the observed turbulence and electron thermal transport. This work was supported by the U.S. Department of Energy under Contracts No. DE-AC02-76CH03073, No. DE-FG03-95ER54295, and No. DE-FG03-99ER54518.

[1] K. W. Gentle et al., Phys. Rev. Lett. 74, 3620 (1995)

[2] Tamura N. et al, Fusion Sci. & Tech., 58, 122 (2010)

[3] K.Ida, private communication (2013)

[4] D. R. Smith et al., Rev. Sci. Instrum. 79, 123501 (2008)

[5] B. P. LeBlanc, Rev. Sci. Instrum. 74, 1659 (2003) and references therein

[6] M. Kotschenreuther et al., Comput. Phys. Commun. 88, 128 (1995).

[7] R. J. Hawryluk, *Physics of Plasma Close to Thermonuclear Conditions* (Pergamon, New York, 1981)